Epipolar Geometry of Central Projection Systems Using Veronese Maps

Joao P. Barreto
ISR/DEEC, University of Coimbra
3030 Coimbra, Portugal
jpbar@deec.uc.pt

Kostas Daniilidis
GRASP Lab., University of Pennsylvania
Philadelphia, PA 19104
kostas@grasp.cis.upenn.edu

Abstract

We study the epipolar geometry between views acquired by mixtures of central projection systems including catadioptric sensors and cameras with lens distortion. Since the projection models are in general non-linear, a new representation for the geometry of central images is proposed. This representation is the lifting through Veronese maps of the image plane to the 5D projective space. It is shown that, for most sensor combinations, there is a bilinear form relating the lifted coordinates of corresponding image points. We analyze the properties of the embedding and explicitly construct the lifted fundamental matrices in order to understand their structure. The usefulness of the framework is illustrated by estimating the epipolar geometry between images acquired by a paracatadioptric system and a camera with radial distortion.

1. Introduction

A central projection camera is an image acquisition device with a single effective viewpoint. The vision sensor measures the intensity of light traveling along rays that intersect in a single point in 3D (the projection center). Examples of broadly used central projection systems are perspective cameras, central catadioptric systems [1], and cameras with lens distortion. The projection in conventional perspective cameras is described by the pin-hole model where scene points are linearly mapped into image points. Corresponding points in two perspective views must satisfy a bilinear constraint that is usually represented by a 3×3 matrix. The fundamental matrix encodes the calibration and rigid displacement between views, and can be estimated in closed-form using image correspondences. These facts make the fundamental geometry one of the most popular and useful concepts in computer vision. Unfortunately, the projection model for central catadioptric systems and cameras with radial distortion is non-linear in homogeneous coordinates. The epipolar geometry between views acquired by mixtures of these systems does no longer have a bilinear form, which considerably limits their usefulness.

The first papers generalizing the epipolar geometry to the non pin-hole case either assumed pre-calibrated systems [13], or completely relied on non-linear iterative minimization [15]. Closely related with the approach herein presented are the works of Geyer et al. [7], Sturm [12] and Claus et al. [5]. Geyer et al. propose an image plane lifting to a four dimensional 'circle space' and prove that there is a 4×4 fundamental matrix encoding the epipolar geometry between two paracatadioptric views. Sturm uses a slightly different lifting strategy and derives the fundamental matrices for mixtures of perspective, affine and paracatadioptric cameras. In [5], Claus et al. propose the lifting of image points to a six dimensional space to build a general purpose model for radial distortion in wide angle and catadioptric lenses. The epipolar geometry between distorted views is represented by a 6×6 matrix. As stated by the authors, their non-parametric model is algebraic in inspiration rather than geometric. Therefore, they do not provide any insight or geometric interpretation about the structure of the lifted fundamental matrix.

In this paper we introduce a representation for the image plane of central systems including catadioptric sensors and cameras with distortion. The representation is similar to the one proposed in [5], and consists in the lifting through Veronese maps of the projective plane $\wp^2$ to the 5D projective space $\wp^5$ [11]. Our goal is to establish a unifying framework for the geometry of general single viewpoint images. A full theory to lift points, lines, conics and conic envelopes is presented. It is also shown how to transfer a linear transformation from $\wp^2$ to $\wp^5$ as well as other geometric relations. We prove that, for most combinations of central projection views, there is a bilinear form relating the lifted coordinates of corresponding points. Our embedding theory is used to understand this lifted epipolar geometry and explicitly construct the different fundamental matrices. The main contributions can be summarized as follows:

- We establish a lifted representation of the image plane and develop a full embedding theory to transfer geometric entities and relations from $\wp^2$ to $\wp^5$.

- We present the lifted fundamental matrices for different mixtures of central projection systems. It is proved for the first time that there is a lifted bilinear constraint between images acquired by a perspective and hyperbolic camera as well as a parabolic sensor and camera with lens distortion.
- The different fundamental matrices are presented in a systematic manner and their structure is discussed. We also provide a comprehensive geometric explanation for the non existence of bilinear forms for hyperbolic views other than the combination with a perspective.

2. Epipolar Geometry using Veronese Maps

Conventional perspective cameras, central catadioptric systems, and cameras with radial distortion are vision systems with a single effective viewpoint. All these sensors measure the intensity of light traveling along rays that intersect in a single point in 3D (the projection center). Consider a coordinate system attached to the camera such that the $\mathbf{R}$ (rotation) and $\mathbf{t}$ (translation) describe its rigid displacement with respect to the world reference frame. Any visible 3D point $\mathbf{X}$ is mapped into a projective ray $\mathbf{x} = \mathbf{PX}$ with $\mathbf{P} = \mathbf{R}[\mathbf{I}| - \mathbf{t}]$. The 3×4 matrix $\mathbf{P}$ is the conventional projection matrix, and we will say that $\mathbf{x} = (x, y, z)^T$ is a projective point in the *Canonical Perspective Plane* (CPP).

Consider the case of central catadioptric systems, where $\mathbf{x}$ is mapped into the image point $\mathbf{x}'$. The relation between these two projective points is provided in equation 1 where $\hbar$ is a non-linear function (equation 2) and $\mathbf{H_c}$ is a collineation depending on the camera intrinsics, the relative rotation between camera and mirror, and the shape of the reflective surface. Function $\hbar$ is equivalent to a projective mapping from a sphere to a plane as shown in Fig. 1 [6]. Parameter ξ in equation 2 depends on the mirror shape and takes values in the interval $]0, 1]$.

$$\mathbf{x}' = \mathbf{H_c}\hbar(\mathbf{x}) \tag{1}$$

$$\hbar(\mathbf{x}) = (x, y, z + \xi\sqrt{x^2 + y^2 + z^2})^T \tag{2}$$

Equation 3 shows the correspondence between projective rays $\mathbf{x}$ and image points $\mathbf{x}'$ for the case of perspective cameras with lens distortion. Matrix $\mathbf{K_c}$ denotes the camera intrinsic parameters and $\eth$ is a non-linear function modeling the radial distortion. In this work the lens distortion is modeled using the division model introduced in [4]. For now we will assume that the coordinates system in the image plane has origin in the distortion center that is known. The inverse function of $\eth$ is provided in equation 4 where parameter ξ quantifies the amount of radial distortion. Transformation $\eth$ has a geometric interpretation similar to the popular sphere model used for catadioptric systems. It can be proved that function $\eth$ is isomorphic to a projective mapping from a paraboloid to a plane (Fig. 1) [2].

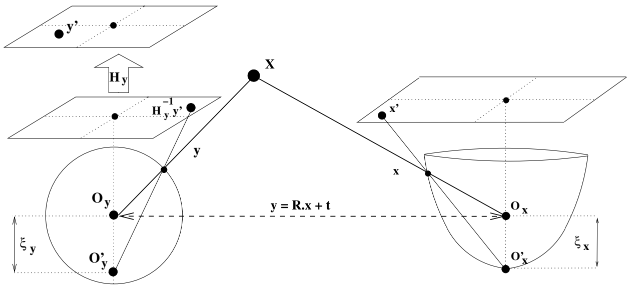

Figure 1. Geometric relation between views acquired by a catadioptric system and a dioptric camera with radial distortion. The 3D point $\mathbf{X}$ is imaged in point $\mathbf{x}'$ in the dioptric camera, and in point $\mathbf{y}'$ in the catadioptric image plane.

$$\mathbf{x}' = \eth(\mathbf{K_c}\mathbf{x}) \tag{3}$$

$$\eth^{-1}(\mathbf{x}') = (x'z', y'z', z'^2 + \xi(x'^2 + y'^2))^T \tag{4}$$

The type of central projection system is defined by the value of parameter ξ. In the case of barrel distortion the ξ is negative and $\eth$ is used. If ξ is positive then the system is a catadioptric sensor. The parameter is unitary in the parabolic case and $\xi \in]0, 1[$ for hyperbolic/elliptical mirrors. For $\xi = 0$ both equations 1 and 2 become linear and represent the well known pin-hole model for perspective cameras.

2.1. Epipolar Geometry

This work aims to study the multi-view relations that hold between images obtained with any mixture of central projection systems. Fig. 1 shows two views of the same 3D point $\mathbf{X}$ acquired by a camera with lens distortion and a central catadioptric sensor. If $\mathbf{x} \leftrightarrow \mathbf{y}$ are corresponding projective rays then they must satisfy $\mathbf{y}^T\mathbf{E}\mathbf{x} = 0$ where $\mathbf{E} = \hat{\mathbf{t}}\mathbf{R}$ is the essential matrix. Since both $\hbar$ and $\eth$ are invertible functions it follows from equations 1 and 2 that

$$\underbrace{(\hbar^{-1}(\mathbf{H_y^{-1}}\mathbf{y}'))}_{\mathbf{y}}{}^T\mathbf{E}\,\underbrace{\mathbf{K_x^{-1}}\eth^{-1}(\mathbf{x}')}_{\mathbf{x}} = 0. \tag{5}$$

It is broadly known that corresponding points in two perspectives satisfy a bilinear constraint called the fundamental equation. The fundamental relation is linear in homogeneous coordinates and can be represented by a 3×3 matrix $\mathbf{F}$. Equation 5 is the equivalent of the fundamental relation for two views acquired by a catadioptric sensor and a camera with distortion. Due to the non-linear image mapping the relation is no longer linear which limits its usefulness when compared with the conventional fundamental matrix.

2.2. Lifting of Coordinates using Veronese Maps

A standard technique used in algebra to render a non-linear problem into a linear one is to find an embedding

	P-H	Hyper.	Parab.	Dist.
P-H	9	1	3	3
Hyper.	1	0	0	0
Parab.	3	0	1	1
Dist.	3	0	1	1

Table 1. Dimension of the null space of matrix $\mathbf{\Psi}$ for pairs of views acquired by different combinations of sensors (*P-H* = pin-hole; *Hyper* = Hyperbolic; *Parab* = Parabolic; *Dist* = Radial Distortion).

that lifts the problem into a higher dimensional space. In a certain extent the homogeneous representation is an embedding of $\Re^2$ into $\Re^3$. Unfortunately the use of an additional coordinate does no longer suffice to cope with the non-linearity of equations 1 and 3. The present work aims to overcome this problem and derive a bilinear fundamental relation that holds for general central projection systems. We propose to embed the projective plane $\wp^2$ in the five dimensional projective space $\wp^5$ using second order Veronese mapping [11]. This polynomial embedding preserves homogeneity and is suitable to deal with quadratic functions because it discriminates the entire set of second order monomials. The lifting of coordinates can be performed by applying the following operator

$$\mathbf{\Gamma}(\mathbf{x}, \bar{\mathbf{x}}) = (x\bar{x}, \frac{x\bar{y} + y\bar{x}}{2}, y\bar{y}, \frac{x\bar{z} + z\bar{x}}{2}, \frac{y\bar{z} + z\bar{y}}{2}, z\bar{z})^T \tag{6}$$

Operator $\mathbf{\Gamma}$ transforms two 3×1 vectors into a 6×1 vector. Equation 6 maps the pair of projective points $\mathbf{x}$, $\bar{\mathbf{x}}$ into one, and only one, point in $\wp^5$. This point lies on a primal of the 5D projective space called the cubic symmetroid [11]. As shown in equation 7, $\mathbf{\Gamma}$ can also be used to map a single point $\mathbf{x}$ into a point $\tilde{\mathbf{x}}$ in the lifted space, lying on a quadratic surface known as the Veronese surface [11]. The Veronese surface $\mathbf{V}$ is a subset of the cubic symmetroid $\mathbf{S}$.

$$\mathbf{x} \longrightarrow \widetilde{\mathbf{x}} = \mathbf{\Gamma}(\mathbf{x}, \mathbf{x}) = (x^2, xy, y^2, xz, yz, z^2)^T. \tag{7}$$

2.3. The Lifted Fundamental Matrix $\digamma$

Fig. 1 shows a pair of corresponding image points $\mathbf{x}' \leftrightarrow \mathbf{y}'$. The lifted coordinates of the two points are $\widetilde{\boldsymbol{x}}'$ and $\widetilde{\boldsymbol{y}}'$ (equation 7). The idea of embedding the projective plane in $\wp^5$ is to obtain a bilinear relation between the two views. The goal is achieved if there is a 6×6 homogeneous matrix $\digamma$ such that

$$\widetilde{\mathbf{y}}'^{\mathbf{T}} \digamma \widetilde{\mathbf{x}}' = 0. \tag{8}$$

Consider the set of lifted correspondences $\widetilde{\mathbf{x}}'_{\mathbf{i}} \leftrightarrow \widetilde{\mathbf{y}}'_{\mathbf{i}}$ with $i = 1, 2 \ldots N$ and $N > 35$. Matrix $\mathbf{\Psi}$ is obtained by stacking the N lines corresponding to the Kronecker products $\widetilde{\mathbf{x}}'^{\mathbf{T}}_{\mathbf{i}} \otimes \widetilde{\mathbf{y}}'^{\mathbf{T}}_{\mathbf{i}}$. The bilinear relation of equation 8 holds *iff* matrix $\mathbf{\Psi}$ is rank deficient. If $\mathbf{\Psi}$ has a left null space then the non-trivial solutions of equation 9 are solutions for the lifted fundamental matrix $\digamma$.

$$\underbrace{\begin{bmatrix} \widetilde{\mathbf{x}}'^{\mathbf{T}}_{\mathbf{1}} \otimes \widetilde{\mathbf{y}}'^{\mathbf{T}}_{\mathbf{1}} \\ \vdots \\ \widetilde{\mathbf{x}}'^{\mathbf{T}}_{\mathbf{N}} \otimes \widetilde{\mathbf{y}}'^{\mathbf{T}}_{\mathbf{N}} \end{bmatrix}}_{\mathbf{\Psi}} \begin{bmatrix} f_{11} \\ \vdots \\ f_{66} \end{bmatrix} = 0 \tag{9}$$

We planned a synthetic experiment to determine the combinations of central projection sensors for which equation 8 holds. For each combination the two vision sensors are placed in a virtual volume and a set of N points is generated assuming a random distribution ($N \gg 35$). Noise free correspondences are obtained by projecting the 3D points in both views. The lifted coordinates of the matching points are used to build matrix $\mathbf{\Psi}$. Tab. 1 summarizes for each case the dimension of the left null space of $\mathbf{\Psi}$. For most of the sensor combinations there is a bilinear relation between views. The only exception is whenever there is an hyperbolic sensor involved. In this situation equation 8 holds only if the other view is acquired by a pin-hole. If one of the views is a conventional perspective then there are multiple solutions for the lifted fundamental matrix.

3. The Embedding in $\wp^5$

In order to interpret the results of Tab. 1 and gain insight about the structure of the lifted fundamental matrix, we need to understand the way that geometric entities and relations in the projective plane are embedded in $\wp^5$.

3.1. Lifting Lines and Conics

A conic curve in $\wp^2$ is usually represented by a 3×3 symmetric matrix $\mathbf{\Omega}$. Point $\mathbf{x}$ lies on $\mathbf{\Omega}$ *iff* equation $\mathbf{x}^T \mathbf{\Omega} \mathbf{x} = 0$ is verified. Since a 3×3 symmetric matrix has 6 parameters, the conic locus can also be represented by a 6×1 homogeneous vector $\widetilde{\boldsymbol{\omega}}$, that is the lifted representation of $\mathbf{\Omega}$ in $\wp^5$ (equation 10).

$$\mathbf{\Omega} = \begin{bmatrix} a & b & d \\ b & c & e \\ d & e & f \end{bmatrix} \longrightarrow \widetilde{\boldsymbol{\omega}} = (a, 2b, c, 2d, 2e, f)^T. \tag{10}$$

Consider the rank 2 conic $\mathbf{\Omega} = \mathbf{m}\mathbf{l}^T + \mathbf{l}\mathbf{m}^T$ composed by two lines $\mathbf{m}$ and $\mathbf{l}$. From equation 10 follows that the corresponding lifted representation is

$$\mathbf{\Omega} = \mathbf{m}\mathbf{l}^T + \mathbf{l}\mathbf{m}^T \longrightarrow \widetilde{\boldsymbol{\omega}} = \widetilde{\mathbf{D}}\mathbf{\Gamma}(\mathbf{m}, \mathbf{l}) \tag{11}$$

where $\widetilde{\mathbf{D}} = diag\{1, 2, 1, 2, 2, 1\}$. A single line $\mathbf{n} = (n_x, n_y, n_z)^T$ is another example of a degenerate conic curve $\mathbf{\Omega} = \mathbf{n}\mathbf{n}^T$. Line $\mathbf{n}$ in the projective plane is mapped into $\widetilde{\mathbf{n}}$ in $\wp^5$ as shown in equation 12.

$$\mathbf{n} \rightarrow \widetilde{\mathbf{n}} = \widetilde{\mathbf{D}}\mathbf{\Gamma}(\mathbf{n},\mathbf{n}) = (n_x^2, 2n_xn_y, n_y^2, 2n_xn_z, 2n_yn_z, n_z^2)^T \quad (12)$$

Conic $\mathbf{\Omega}$ goes through point $\mathbf{x}$ *iff* the inner product of the corresponding lifted representations is zero ($\mathbf{x}^T\mathbf{\Omega}\mathbf{x} = 0 \rightarrow \widetilde{\boldsymbol{\omega}}^T\widetilde{\mathbf{x}} = 0$). Additionally, if points $\mathbf{x}$ and $\bar{\mathbf{x}}$ are harmonic conjugates with respect to $\mathbf{\Omega}$, then $\widetilde{\boldsymbol{\omega}}^{\mathbf{T}}\mathbf{\Gamma}(\mathbf{x},\bar{\mathbf{x}}) = 0$. The embedding of the projective plane in $\wp^{\mathbf{5}}$ using Veronese mapping creates a dual relation between points and conics. Moreover, and since lines are degenerate conics of rank 1, the duality between points and lines is preserved.

3.2. Lifting Conic Envelopes

In general a point conic $\mathbf{\Omega}$ has a dual conic envelope $\mathbf{\Omega}^*$ associated with it [11]. The envelope is usually represented by a 3×3 symmetric matrix. A certain line $\mathbf{n}$ is on the conic envelope whenever it satisfies $\mathbf{n}^T\mathbf{\Omega}^*\mathbf{n} = 0$. The conic envelope can also be represented by a 6×1 homogeneous vector $\widetilde{\boldsymbol{\omega}}^*$ (equation 13). In this case a line $\mathbf{n}$ lies on $\mathbf{\Omega}^*$ *iff* the corresponding lifted vectors $\widetilde{\mathbf{n}}$ and $\widetilde{\boldsymbol{\omega}}^*$ are orthogonal.

$$\mathbf{\Omega}^* = \begin{bmatrix} a^* & b^* & d^* \\ b^* & c^* & e^* \\ d^* & e^* & f^* \end{bmatrix} \longrightarrow \widetilde{\boldsymbol{\omega}}^* = (a^*, b^*, c^*, d^*, e^*, f^*)^T. \quad (13)$$

If matrix $\mathbf{\Omega}^*$ is rank deficient then the conic envelope is said to be degenerate. There are two possible cases of degeneracy: when the $\mathbf{\Omega}^*$ is composed by two pencils of lines going through points $\mathbf{x}$ and $\bar{\mathbf{x}}$ ($\mathbf{\Omega}^* = \mathbf{x}\bar{\mathbf{x}}^T + \bar{\mathbf{x}}\mathbf{x}^T$), and when the envelope is formed by a single pencil of lines ($\mathbf{\Omega}^* = \mathbf{x}\mathbf{x}^T$). The lifted representations are respectively provided in equations 14 and 15.

$$\mathbf{\Omega}^* = \mathbf{x}\bar{\mathbf{x}}^T + \bar{\mathbf{x}}\mathbf{x}^T \longrightarrow \widetilde{\boldsymbol{\omega}}^* = \mathbf{\Gamma}(\mathbf{x},\bar{\mathbf{x}}) \quad (14)$$

$$\mathbf{\Omega}^* = \mathbf{x}\mathbf{x}^T \longrightarrow \widetilde{\boldsymbol{\omega}}^* = \mathbf{\Gamma}(\mathbf{x},\mathbf{x}) \quad (15)$$

3.3. Lifting Linear Transformations

The linear transformation $\mathbf{H}$ maps points $\mathbf{x}$ and $\bar{\mathbf{x}}$ in points $\mathbf{H}\mathbf{x}$ and $\mathbf{H}\bar{\mathbf{x}}$. The operator $\mathbf{\Lambda}$, that lifts transformation $\mathbf{H}$ from the projective plane to the embedding space $\wp^{\mathbf{5}}$, must satisfy the following relation

$$\mathbf{\Gamma}(\mathbf{H}\mathbf{x},\mathbf{H}\bar{\mathbf{x}}) = \mathbf{\Lambda}(\mathbf{H}).\mathbf{\Gamma}(\mathbf{x},\bar{\mathbf{x}}) \quad (16)$$

Such operator can be derived by algebraic manipulation.

$$\mathbf{\Lambda}(\underbrace{[\,\mathbf{v_1}\ \mathbf{v_2}\ \mathbf{v_3}\,]}_{\mathbf{H}}) = \underbrace{[\,\mathbf{\Gamma_{11}}\mathbf{\Gamma_{12}}\mathbf{\Gamma_{22}}\mathbf{\Gamma_{13}}\mathbf{\Gamma_{23}}\mathbf{\Gamma_{33}}\,]\,\widetilde{\mathbf{D}}}_{\widetilde{\mathbf{H}}} \quad (17)$$

It can be proved that the operator provided above verifies the following properties

$$\begin{array}{rcl} \mathbf{\Lambda}(\mathbf{H}^{-1}) & = & \mathbf{\Lambda}(\mathbf{H})^{-1} \\ \mathbf{\Lambda}(\mathbf{H}.\mathbf{B}) & = & \mathbf{\Lambda}(\mathbf{H}).\mathbf{\Lambda}(\mathbf{B}) \\ \mathbf{\Lambda}(\mathbf{H}^T) & = & \widetilde{\mathbf{D}}^{-1}.\mathbf{\Lambda}(\mathbf{H})^T.\widetilde{\mathbf{D}} \\ \mathbf{\Lambda}(\mathbf{I}_{3\times3}) & = & \mathbf{I}_{6\times6} \end{array} \quad (18)$$

Operator $\mathbf{\Lambda}$ maps any 3×3 matrix $\mathbf{H}$ into a 6×6 matrix $\widetilde{\mathbf{H}}$. A pair of points in the plane is related by $\mathbf{H}$, *iff* the pair of corresponding lifted representations in $\wp^{\mathbf{5}}$ is related by $\widetilde{\mathbf{H}}$ ($\mathbf{y} = \mathbf{H}\mathbf{x} \leftrightarrow \widetilde{\mathbf{y}} = \widetilde{\mathbf{H}}\widetilde{\mathbf{x}}$). The set of transformations $\widetilde{\mathbf{H}} = \mathbf{\Lambda}(\mathbf{H})$ is the subset of linear transformations of $\wp^{\mathbf{5}}$ that fixes both the cubic symmetroid $\mathbf{S}$ and the Veronese surface $\mathbf{V}$. However, neither $\mathbf{S}$ nor $\mathbf{V}$ are fixed point-wise. The transformation of points, conics and conic envelopes are lifted in the following manner

$$\begin{array}{lcl} \mathbf{y} = \mathbf{H}\mathbf{x} & \longrightarrow & \widetilde{\mathbf{y}} = \widetilde{\mathbf{H}}\widetilde{\mathbf{x}} \\ \mathbf{\Psi} = \mathbf{H}^{-T}\mathbf{\Omega}\mathbf{H}^{-1} & \longrightarrow & \widetilde{\psi} = \widetilde{\mathbf{H}}^{-T}\widetilde{\omega} \\ \mathbf{\Psi}^* = \mathbf{H}\mathbf{\Omega}^*\mathbf{H}^T & \longrightarrow & \widetilde{\psi}^* = \widetilde{\mathbf{H}}\widetilde{\omega}^* \end{array} \quad (19)$$

The operator $\mathbf{\Lambda}$ can be also be applied to lift correlations in $\wp^{\mathbf{2}}$ [11]. A correlation $\mathbf{G}$ maps points $\mathbf{x}$ into lines $\mathbf{n} = \mathbf{G}\mathbf{x}$. It can been easily proved that the corresponding lifted coordinates are related by $\widetilde{\mathbf{n}} = \widetilde{\mathbf{D}}\widetilde{\mathbf{G}}\widetilde{\mathbf{x}}$.

4. Useful Relations in $\wp^{\mathbf{5}}$

The previous section shows how a linear transformation in the original space $\wp^{\mathbf{2}}$ can be transferred to a linear transformation in $\wp^{\mathbf{5}}$. This section focuses on the non-linear features of the mapping functions of equations 1 and 3. Therefore, and without loss of generality, collineations $\mathbf{H_c}$ and $\mathbf{K_c}$ will be ignored for clarity reasons.

The catadioptric projection of a line is in general a conic curve [13, 6]. This is due to the non-linear characteristics of function $\hbar$ (equation 2) that transforms points $\mathbf{x}$ in the *Canonical Perspective Plane* (CPP) into image points $\mathbf{x}'$. We show that there is a linear correspondence between the lifted representation of a line $\mathbf{n}$ and the conic curve where it is projected. This result allows us to derive a linear relation between an image point $\mathbf{x}'$ and its back-projections in the CPP. The discussion of the this section is of key importance to interpret the results of Tab. 1.

4.1. Projection of Lines

Consider the central catadioptric sensor depicted in Fig. 1 and a plane $\mathbf{\Pi}$ defined by a 3D line and the system effective viewpoint $\mathbf{O}$. The normal vector of $\mathbf{\Pi}$ is $\mathbf{n} = (n_x, n_y, n_z)^T$ that can also be interpreted has a line projection in the CPP. Plane $\mathbf{\Pi}$ intersects the reference sphere in a great circle that is projected from $\mathbf{O}'$ into a conic curve $\mathbf{\Omega}'$. The non-linear formula relating a line $\mathbf{n}$ in the CPP and the image conic $\mathbf{\Omega}'$ is provided in [6]. If $\widetilde{\mathbf{n}}$ and $\widetilde{\boldsymbol{\omega}}'$ are the

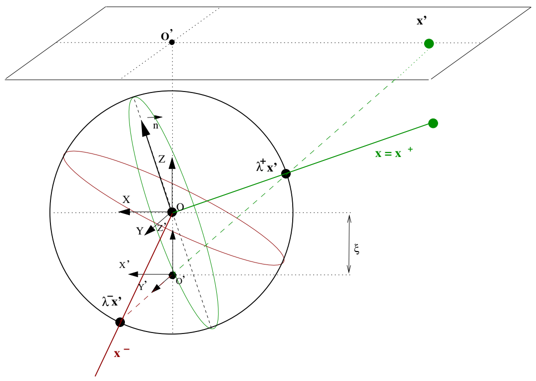

Figure 2. Back-projection of points in an hyperbolic sensor. The projective ray associated with $\mathbf{x}'$ intersects the unitary sphere in two points. These points define two distinct back-projections $\mathbf{x}^+$ (forward looking direction) and $\mathbf{x}^-$ (backward looking direction)

lifted coordinates of $\mathbf{n}$ and $\mathbf{\Omega}'$ then it is straightforward to prove that equation 20 holds. The 6×6 matrix $\widetilde{\mathbf{\Delta}}_{\boldsymbol{c}}$ of equation 21 transforms a line in the CPP into the corresponding conic curve in the catadioptric image plane. Remark that the structure of $\widetilde{\mathbf{\Delta}}_{\boldsymbol{c}}$ does not follow equation 17, which means that there is no linear counterpart in $\wp^{\mathbf{2}}$.

$$\widetilde{\boldsymbol{\omega}}' = \widetilde{\mathbf{\Delta}}_{\boldsymbol{c}}\widetilde{\mathbf{n}}. \tag{20}$$

$$\widetilde{\mathbf{\Delta}}_{\boldsymbol{c}} = \begin{bmatrix} 1-\xi^2 & 0 & 0 & 0 & 0 & -\xi^2 \\ 0 & 1-\xi^2 & 0 & 0 & 0 & 0 \\ 0 & 0 & 1-\xi^2 & 0 & 0 & -\xi^2 \\ 0 & 0 & 0 & 1 & 0 & 0 \\ 0 & 0 & 0 & 0 & 1 & 0 \\ 0 & 0 & 0 & 0 & 0 & 1 \end{bmatrix} ; \widetilde{\mathbf{\Delta}}_{\boldsymbol{r}} = \begin{bmatrix} 0 & 0 & 0 & 0 & 0 & \xi \\ 0 & 0 & 0 & 0 & 0 & 0 \\ 0 & 0 & 0 & 0 & 0 & \xi \\ 0 & 0 & 0 & 0.5 & 0 & 0 \\ 0 & 0 & 0 & 0 & 0.5 & 0 \\ 0 & 0 & 0 & 0 & 0 & 1 \end{bmatrix} \tag{21}$$

The projection of a line by a camera with lens distortion is also a conic curve. Function $\eth$ of equation 4 is equivalent to projecting the scene on the surface of an unitary paraboloid and re-projecting from its vertex. As shown in Fig. 1 a projective ray $\mathbf{x}$ going through the camera projection center $\mathbf{O}$ is mapped in $\mathbf{x}'$ going through $\mathbf{O}'$. In this case plane $\mathbf{\Pi}$, containing the original 3D line, cuts the reference paraboloid in a great circle that is projected into a conic $\mathbf{\Omega}'$. The lifted representations of the line $\mathbf{n}$ in the CPP and the image conic are linearly related in $\wp^{\mathbf{5}}$ by $\widetilde{\boldsymbol{\omega}}' = \widetilde{\mathbf{\Delta}}_{\boldsymbol{r}}\widetilde{\mathbf{n}}$. The 6×6 matrix $\widetilde{\mathbf{\Delta}}_{\boldsymbol{r}}$ is provided in equation 21 where ξ quantifies the amount of radial distortion.

4.2. Back-Projection of Image Points in Central Catadioptric Systems

Fig. 2 shows the sphere model for a catadioptric sensor. A 3D point $\mathbf{X}$ defines a projective ray/point $\mathbf{x}$ that is mapped at $\mathbf{x}' = \hbar(\mathbf{x})$. Given an image point $\mathbf{x}' = (x', y', z')^T$, we intend to invert the mapping in order to compute its back-projection $\mathbf{x}$ in the CPP. The equation of the reference sphere in the coordinates system centered in $\mathbf{O}'$ is $x'^2 + y'^2 + (z' - \xi)^2 = 1$. Since $\mathbf{x}'$ is a projective ray going through $\mathbf{O}'$, there is a scalar λ such that $\lambda\mathbf{x}'$ is a 3D point lying on the sphere surface. The scalar λ can be computed by solving equation $(\lambda x')^2 + (\lambda y')^2 + (\lambda z' - \xi)^2 = 1$. Since it is a second order equation, there are two solutions λ^+ and λ^- that are provided below.

$$\lambda^\pm = \frac{z'\xi \pm \sqrt{z'^2 + (1-\xi^2)(x'^2 + y'^2)}}{x'^2 + y'^2 + z'^2} \tag{22}$$

The projective ray $\mathbf{x}'$, with origin in $\mathbf{O}'$, intersects the reference sphere in two points $\lambda^+\mathbf{x}'$ and $\lambda^-\mathbf{x}'$ (Fig. 2). By representing these points in the reference frame centered in the effective viewpoint $\mathbf{O}$ we obtain two distinct back-projections $\mathbf{x}^+$ and $\mathbf{x}^-$ (equation 23). Since the camera is forward looking the mirror, the correct solution for the back-projection is $\mathbf{x} = \mathbf{x}^+$. Point $\mathbf{x}^-$ is just a spurious algebraic solution.

$$\mathbf{x}^\pm = (\lambda^\pm x', \lambda^\pm y', \lambda^\pm z' - \xi)^T \tag{23}$$

Assume a line $\mathbf{n}$ in the CPP going through one of the back-projections of $\mathbf{x}'$. Line $\mathbf{n}$ is projected into a conic curve $\mathbf{\Omega}'$ that must go through the image point $\mathbf{x}'$. Therefore, and considering the embedding in $\wp^{\mathbf{5}}$, it follows that $\widetilde{\boldsymbol{\omega}}'^T\widetilde{\mathbf{x}}' = 0$. Replacing $\widetilde{\boldsymbol{\omega}}'$ by the result of equation 20 yields

$$\widetilde{\mathbf{n}}^T \underbrace{\widetilde{\mathbf{\Delta}}_{\boldsymbol{c}}^T \widetilde{\mathbf{x}}'}_{\widetilde{\boldsymbol{\omega}}*} = 0. \tag{24}$$

Equation 24 is satisfied by any line $\mathbf{n}$ going through one of the back-projections of $\mathbf{x}'$ which means that $\widetilde{\boldsymbol{\omega}}^*$ is the lifted representation of a the conic envelope in the CPP. The conic envelope is degenerate (rank 2) because it is composed by two pencils of lines defined by points $\mathbf{x}^+$ and $\mathbf{x}^-$. Equation 25 is derived taking into account that $\widetilde{\boldsymbol{\omega}}^* = \mathbf{\Gamma}(\mathbf{x}^+, \mathbf{x}^-)$ (equation 14). The embedding in $\wp^{\mathbf{5}}$ allowed us to establish a linear relation between a point in the catadioptric image plane and the corresponding back-projections in the CPP.

$$\mathbf{\Gamma}(\mathbf{x}^+, \mathbf{x}^-) = \widetilde{\mathbf{\Delta}}_{\boldsymbol{c}}^T \widetilde{\mathbf{x}}'. \tag{25}$$

4.3. Back-Projection of Image Points in Paracatadioptric Systems and Cameras with Distortion

For the case of paracatadioptric systems the parameter ξ is unitary and the projective mapping of Fig. 2 becomes a stereographic projection [6]. If $\xi = 1$ then $\lambda^- = 0$ and the spurious back-projection is always $\mathbf{x}^- = (0, 0, 1)^T$ (equations 22 and 23). Since the re-projection center is on the sphere, the projective ray $\mathbf{x}'$ must always intersect the surface in $\mathbf{O}'$ which explains the result. Assume that the back-projection in the forward-looking direction is $\mathbf{x} = (x, y, z)$ ($\mathbf{x}^+ = \mathbf{x}$). Since $\mathbf{\Gamma}(\mathbf{x}^+, \mathbf{x}^-) = (0, 0, 0, x/2, y/2, z)^T$, it follows from equation 25 that

	Pin-Hole	Hyperbolic	Parabolic	Distortion
Pin-Hole	$\mathbf{K_y^{-T} E K_x^{-1}}$	$\mathbf{\widetilde{K}_y^{-T} \widetilde{D} \widetilde{E} \widetilde{\Delta}_c^{\mathit{T}} \widetilde{H}_x^{-1}}$	$\mathbf{K_y^{-T} E \Theta^{\mathit{T}} \widetilde{H}_x^{-1}}$	$\mathbf{K_y^{-T} E K_x^{-1} \widetilde{\Phi}_{\mathit{x}}^{\mathit{T}}}$
Hyperbolic	$\mathbf{\widetilde{H}_y^{-T} \widetilde{\Delta}_{\mathit{c}} \widetilde{D} \widetilde{E} \widetilde{K}_x^{-1}}$	-	-	-
Parabolic	$\mathbf{\widetilde{H}_y^{-T} \Theta E K_x^{-1}}$	-	$\mathbf{\widetilde{H}_y^{-T} \Theta E \Theta^{\mathit{T}} \widetilde{H}_x^{-1}}$	$\mathbf{\widetilde{H}_y^{-T} \Theta E K_x^{-1} \Phi_{\mathit{x}}^{\mathit{T}}}$
Distortion	$\mathbf{\Phi_{\mathit{y}} K_y^{-T} E K_x^{-1}}$	-	$\mathbf{\Phi_{\mathit{y}} K_y^{-T} E \Theta^{\mathit{T}} \widetilde{H}_x^{-1}}$	$\mathbf{\Phi_{\mathit{y}} K_y^{-T} E K_x^{-1} \Phi_{\mathit{x}}^{\mathit{T}}}$

Table 2. This table summarizes the results for the lifted fundamental matrices $\mathcal{F}$ relating pairs of views acquired by any mixture of central projection systems. The perspective image plane should not be lifted to avoid multiple solutions for the fundamental geometry (see Tab. 1). Therefore, $\mathcal{F}$ is a 3×3 matrix in the case of two pin-hole images, and a 3×6 matrix for the situation of a perspective view and a paracatadioptric/distortion view. In the remaining cases $\mathcal{F}$ is always a 6×6 square matrix.

$$\mathbf{x} = \underbrace{\begin{bmatrix} 2 & 0 & 0 \\ 0 & 2 & 0 \\ 0 & 0 & 1 \end{bmatrix} \begin{bmatrix} 0 & 0 & 0 & 1 & 0 & 0 \\ 0 & 0 & 0 & 0 & 1 & 0 \\ -1 & 0 & -1 & 0 & 0 & 1 \end{bmatrix}}_{\mathbf{\Theta}^T} \widetilde{\mathbf{x}}'. \tag{26}$$

According to equation 26 there is a linear transformation that maps the lifted coordinates of a point in the paracatadioptric image into the corresponding point $\mathbf{x}$ in the CPP. Remark that the 3×6 matrix is the transpose of the three last columns of $\widetilde{\mathbf{\Delta}}_c$ when $\xi = 1$ (equation 21).

For the case of cameras with lens distortion the re-projection center is located on the vertex of the paraboloid (Fig. 1). This case is similar to the paracatadioptric system because $\mathbf{O}'$ also lies on the reference surface. The spurious back-projection $\mathbf{x}^-$ is always $(0, 0, \xi)$, and there is a 3×6 matrix $\mathbf{\Phi}^T$ that maps lifted image points $\widetilde{\mathbf{x}}'$ into points $\mathbf{x} = \eth^{-1}(\mathbf{x}')$.

$$\mathbf{x} = \underbrace{\begin{bmatrix} 2 & 0 & 0 \\ 0 & 2 & 0 \\ 0 & 0 & 1 \end{bmatrix} \begin{bmatrix} 0 & 0 & 0 & 0.5 & 0 & 0 \\ 0 & 0 & 0 & 0 & 0.5 & 0 \\ \xi & 0 & \xi & 0 & 0 & 1 \end{bmatrix}}_{\mathbf{\Phi}^T} \widetilde{\mathbf{x}}' \tag{27}$$

5. Fundamental Matrices in $\wp^5$

In the experiment of section 2.3 we artificially generated a set of noise-free correspondences and investigated the dimensionality of the null space of matrix $\mathbf{\Psi}$ to find the mixtures of central projection systems with a fundamental matrix in lifted coordinates. The results of Tab. 1 are a good guideline, however they do not provide a geometric insight on the problem. In this section we apply the embedding theory presented in sections 3 and 4 to explicitly derive the lifted fundamental matrices.

5.1. Views Acquired by Pin-Hole Cameras

Consider two views acquired by a pair of perspective cameras with intrinsic parameters $\mathbf{K_x}$ and $\mathbf{K_y}$. Corresponding image points $\mathbf{x}' \leftrightarrow \mathbf{y}'$ must satisfy $\mathbf{y}'^T \mathbf{F} \mathbf{x}' = 0$ with $\mathbf{F}$ the conventional 3×3 fundamental matrix. $\mathbf{F}$ is a correlation in the projective plane because it transforms points in one view into lines in the other view (the epipolar lines). According to section 3.3, a correlation $\mathbf{F}$ in $\wp^2$ is lifted to $\widetilde{\mathbf{D}}\widetilde{\mathbf{F}}$ in the 5D projective space. Taking into account the result of equation 18, it follows that

$$\mathbf{F} = \mathbf{K_y^{-T} E K_x^{-1}} \quad \longrightarrow \quad \widetilde{\mathbf{D}}\widetilde{\mathbf{F}} = \widetilde{\mathbf{K}}_\mathbf{y}^{-\mathbf{T}} \widetilde{\mathbf{D}} \widetilde{\mathbf{E}} \widetilde{\mathbf{K}}_\mathbf{x}^{-1} \tag{28}$$

The experiment of section 2.3 confirms that if $\mathbf{y}'^T \mathbf{F} \mathbf{x}' = 0$ then $\widetilde{\mathbf{y}}'^{\mathbf{T}} \widetilde{\mathbf{D}} \widetilde{\mathbf{F}} \widetilde{\mathbf{x}}' = 0$. Matrix $\mathcal{F} = \widetilde{\mathbf{D}}\widetilde{\mathbf{F}}$ is a lifted fundamental matrix relating two views acquired by perspective cameras. However there are other solutions for equation 9. It is easy to see that the following equation holds

$$\widetilde{\mathbf{y}}'^{\mathbf{T}} \left[\begin{smallmatrix} \mathbf{0} & \mathbf{0} \\ \mathbf{0} & \mathbf{F} \end{smallmatrix}\right] \widetilde{\mathbf{x}}' = 0.$$

Tab. 1 shows that the null space of matrix $\mathbf{\Psi}$ is multi-dimensional. For the case of image pairs acquired by pin-hole cameras the epipolar geometry is described by a bilinear form in $\wp^2$. Since there is a fundamental matrix $\mathbf{F}$, the lifting to $\wp^5$ is just an over parameterization that leads to multiple $\mathcal{F}$ solutions.

5.2. Views Acquired by Paracatadioptric Sensors and Cameras with Radial Distortion

Consider the scheme of Fig. 1 showing a camera with lens distortion and a paracatadioptric system. The projection centers are respectively $\mathbf{O_x}$ and $\mathbf{O_y}$, $\mathbf{K_x}$ represents the intrinsic parameters of the dioptric camera (equation 3), and $\mathbf{H_y}$ encodes the calibration of the paracatadioptric sensor (equation 1). The 3D point $\mathbf{X}$ defines two projective rays, $\mathbf{x}$ and $\mathbf{y}$, going through the effective viewpoints $\mathbf{O_x}$ and $\mathbf{O_y}$. The two points verify $\mathbf{y}^T \mathbf{E} \mathbf{x} = 0$ where $\mathbf{E}$ stands for the conventional essential matrix. Point $\mathbf{x}$ is mapped in the distorted image plane at $\mathbf{x}' = \eth(\mathbf{K_x x})$ (equation 3). From equation 27 follows that $\mathbf{x} = \mathbf{K_x^{-1}} \mathbf{\Phi}_x^T \widetilde{\mathbf{x}}'$. The projection in the paracatadioptric image plane is $\mathbf{y}' = \mathbf{H_y} \hbar(\mathbf{y})$ and the inverse mapping is $\mathbf{y} = \mathbf{\Theta}^T \widetilde{\mathbf{H}}_\mathbf{y}^{-1} \widetilde{\mathbf{y}}'$ (equations 1, 17, 18 and 26). Replacing $\mathbf{x}$ and $\mathbf{y}$ in the essential relation yields

$$\widetilde{\mathbf{y}}'^{\mathbf{T}} \underbrace{\widetilde{\mathbf{H}}_\mathbf{y}^{-\mathbf{T}} \mathbf{\Theta} \mathbf{E} \mathbf{K_x^{-1}} \mathbf{\Phi}_{\boldsymbol{x}}^{\boldsymbol{T}}}_{\mathcal{F}} \widetilde{\mathbf{x}}' = 0 \tag{29}$$

The derived matrix $\mathcal{F}$ is the 6×6 fundamental matrix observed in section 2.3 for the mixture of distorted and paracatadioptric views. Remark that $\mathcal{F}$ is still a correlation in $\wp^5$, transforming the lifted coordinates of points in one view into the corresponding epipolar curves in the other view ($\widetilde{\omega}'_y = \mathcal{F}\widetilde{\mathbf{x}}'$ and $\widetilde{\omega}'_x = \mathcal{F}^T\widetilde{\mathbf{y}}'$). The reasoning to derive the lifted fundamental matrices for mixtures of two paracatadioptric sensors and two cameras with radial distortion is similar. The results are presented in Tab. 2.

For views acquired by a parabolic sensor and a pin-hole camera there are multiple 6×6 fundamental matrices $\mathcal{F}$ satisfying equation 8 (Tab. 1). As discussed above, by lifting the point coordinates in a perspective image we end up with an over-parameterization that generates multiple solutions. The problem is solved by using lifted coordinates only for the paracatadioptric view. Equation 30 shows the corresponding 3×6 fundamental matrix. The case of a pinhole and a camera with lens distortion is identical.

$$\mathbf{y}'^{\mathbf{T}} \underbrace{\mathbf{K_y^{-T}}\mathbf{E}\mathbf{\Theta}^T\widetilde{\mathbf{H}}_{\mathbf{x}}^{-1}}_{\mathcal{F}_{3\times 6}} \widetilde{\mathbf{x}}' = 0 \quad (30)$$

The division model is a simple second order model that requires the center to be known and the distortion to be isotropic [10]. There are other distortion models without such limitations [14, 8]. Remark that our framework can be used with any non-linear projection model, as far as there is a 3×6 linear transformation between lifted image coordinates and undistorted points (equation 27).

5.3. Views Acquired by Hyperbolic Sensors

According to the synthetic experiment of section 2.3, the lifting of coordinates fails in enforcing a bilinear form for the epipolar geometry of mixtures that include hyperbolic sensors. As explained in section 4.2, the lifted representation of an image point $\widetilde{\mathbf{x}}'$ can be mapped by a linear transformation into a conic envelope that encodes the correct back-projection $\mathbf{x} = \mathbf{x}^+$, and a spurious solution $\mathbf{x}^-$. For the case of paracatadioptric systems and cameras with lens distortion the spurious solution is constant and there is a linear transformation that maps $\widetilde{\mathbf{x}}'$ in $\mathbf{x}$. The results of equations 26 and 27 proved to be crucial in deriving the lifted fundamental matrices for mixtures involving these systems. For the case of hyperbolic sensors it is not possible to decouple $\mathbf{x}^-$ and $\mathbf{x}^+$, which explains the non existence of fundamental matrices. One possible solution is to increase the dimensionality of the Veronese lifting. However, the corresponding estimation problem would probably be non tractable. An alternative is to find an embedding that simultaneously encodes orientation and preserves homogeneity. Such embedding, as far as we are aware, does not exist.

The only case that admits a lifted fundamental matrix is the combination with a perspective view. The structure of the corresponding 6×6 fundamental matrix $\mathcal{F}$ is provided in equation 31. Curiously, the epipolar curve in the perspective plane $\widetilde{\omega}'_y = \mathcal{F}\widetilde{\mathbf{x}}'$ is a rank 2 conic. This conics is composed by two lines: the forward looking epipolar line and the backward looking epipolar line.

$$\widetilde{\mathbf{y}}'^{\mathbf{T}} \underbrace{\widetilde{\mathbf{K}}_{\mathbf{y}}^{-\mathbf{T}}\widetilde{\mathbf{D}}\widetilde{\mathbf{E}}\widetilde{\mathbf{\Delta}}_c^T\widetilde{\mathbf{H}}_{\mathbf{x}}^{-1}}_{\mathcal{F}} \widetilde{\mathbf{x}}' = 0 \quad (31)$$

6. Experiments with Real Images

Tab. 2 shows the mixtures of central projection systems for which there are lifted bilinear constraints between views. For these cases, and under the assumption of an ideal noise-free situation, the computation of the fundamental matrix $\mathcal{F}$ from a set of image correspondences is straightforward. As shown in equation 9, we just need to build matrix $\mathbf{\Psi}$ and determine its right null space. In practice the correspondences are always affected by noise and matrix $\mathbf{\Psi}$ is in general full rank. In this situation we can always apply SVD decomposition to enforce a null space and estimate $\mathcal{F}$. The problem is that not every 6×6 matrix is a lifted fundamental matrix. As discussed in the previous section, $\mathcal{F}$ must be a rank 2 matrix with a specific structure that depends on the type of central cameras used to acquire the views (Tab. 2). In [5], Claus et al. report an experiment in estimating the fundamental matrix between two views acquired with a fish-eye lens using a standard linear algorithm. According to the report, they succeeded in obtaining a bilinear form that seems to fit the data, however they were unable to extract correct distortion information. This suggests that the use of purely algebraic approaches is not enough, and that the structure of $\mathcal{F}$ must be taken into account.

To prove the applicability of our framework we ran an experiment to estimate the geometry between two uncalibrated images acquired by a paracatadioptric system and a camera with lens distortion (Fig. 3). The estimation problem is simplified by considering a skewless parabolic system with unitary aspect ratio. Under this assumption the lifting of coordinates is similar to the one used in [7, 12], and the dimension of $\mathcal{F}$ is 4×4. From the correspondences we build a matrix $\mathbf{\Psi}$ (equation 9) and estimate $\mathcal{F}$ using linear least squares. The rank constraint on $\mathcal{F}$ is enforced using SVD. From the analysis of the structure of $\mathcal{F}$ it follows that the null space on the side of the distorted view encodes the undistorted epipole and the amount of distortion. This information is extracted and used as a prior to re-fit the matrix to the correspondences. The sub-optimal two step factorization approach is entirely linear and provides a fundamental matrix with the desired structure (for further details see [3]). Since the estimation has a closed-form solution, it can be run in a RANSAC approach to discard outliers. Fig. 3 shows the results in estimating the lifted fundamental ma-

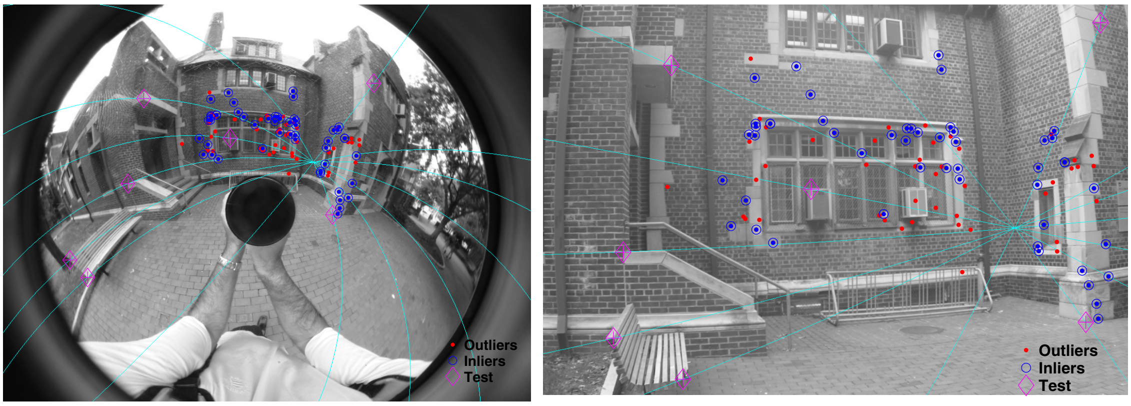

Figure 3. Estimation of the lifted fundamental matrix for views acquired by a paracatadioptric sensor and a camera with radial distortion. The Lowe's detector found 101 correspondences from which 54 were marked as inliers. The high rejection percentage is explained by the difficulty in establishing robust correspondences between images that look so different.

trix. The correspondences were automatically detected using SIFT features [9]. To test the correctness of the result we manually selected 7 correspondences and drew the corresponding epipolar curves (Fig. 3). Additionally we extracted the radial distortion information from the estimated F and corrected the distorted view (Fig. 4).

7. Conclusions

We proposed a representation for central projection images through a lifting of the projective plane to the 5D projective space. In addition, we presented a full embedding theory to transfer geometric entities and relations between the original and lifted spaces. The theory was applied to explicitly construct the lifted fundamental matrices and understand their structure. We believe that such geometric insight is essential to develop robust estimation algorithms and extract information from the estimated matrices.

Acknowledgments

The authors are grateful for support through grants NSF-IIS-0121293, NSF-EIA-0324977, NSF-CNS-0423891, NSF-IIS-0431070, and ARO/MURI DAAD19-02-1-0383. They also acknowledge the generous funding from the Luso-American Foundation for Development, and the useful help of Jose Roquette with the experiments.

Figure 4. Correction of the Radial Distortion in a 853×1280 image. The estimated distortion was 145.7 pixels at the image corner

References

[1] S. Baker and S. Nayar. A theory of catadioptric image formation. In *Proc. of ICCV*, 1998.

[2] J. P. Barreto and K. Daniilidis. Unifying liftings for catadioptric and dioptric cameras. In *Proc. of OMNIVIS*, 2004.

[3] J. P. Barreto and K. Daniilidis. Fundamental matrix for cameras with radial distortion. In *Proc. of ICCV*, 2005.

[4] C. Brauer-Burchardt and K. Voss. A new algorithm to correct fish-eye- and strong wide-angle- lens-distortion from single images. In *Proc. of ICIP*, 2001.

[5] D. Claus and A. Fitzgibbon. A rational function for fish-eye lens distortion. In *Proc. of CVPR*, 2005.

[6] C. Geyer and K. Daniilidis. A unifying theory for central panoramic systems. In *Proc. of ECCV*, 2000.

[7] C. Geyer and K. Daniilidis. Structure and motion from uncalibrated catadioptric views. In *Proc. of CVPR*, 2001.

[8] R. Hartley and S. B. Kang. Parameter-free radial distortion correction with center of distortion estimation. In *Proc. of ICCV*, 2005.

[9] D. Lowe. Distinctive image features from scale-invariant keypoints. *IJCV*, 2004.

[10] B. Micusik and T. Padjla. Estimation of omnidirectional camera model from epipolar geometry. In *Proc. of CVPR*, 2003.

[11] J. G. Sample and G. T. Kneebone. *Algebraic Projective Geometry*. Claredon Press, 1998.

[12] P. Sturm. Mixing catadioptric and perspective cameras. In *Proc. of OMNIVIS*, 2002.

[13] T. Svoboda and T. Pajdla. Epipolar geometry for central catadioptric cameras. *IJCV*, August 2002.

[14] S. Thirthala and M. Pollefeys. The radial trifocal tensor: A tool for calibrating radial distortion of wide-angle cameras. In *Proc. of CVPR*, 2005.

[15] Z. Zhang. On the epipolar geometry between two images with lens distortion. In *Proc. of ICPR*, 1996.